Climatology and Trends in Concurrent Temperature Extremes in the Global Extratropics

Gabriele Messori[1,2], Antonio Segalini[1], Alexandre M. Ramos[3]

[1] Department of Earth Sciences and Swedish Centre for Impacts of Climate Extremes (CLIMES), Uppsala University, Uppsala, Sweden.
[2] Department of Meteorology and Bolin Centre for Climate Research, Stockholm University, Stockholm, Sweden.
[3] Institute of Meteorology and Climate Research, Karlsruhe Institute of Technology, Karlsruhe, Germany.

Correspondence to: Gabriele Messori (gabriele.messori@geo.uu.se)

Abstract. Simultaneous occurrences of multiple heatwaves or cold spells in remote geographical regions have drawn considerable attention in the literature, due to their potentially far-reaching impacts. We introduce a flexible toolbox to study such concurrent temperature extremes, with adjustable parameters that different users can tailor to their specific needs. We then use the toolbox to present a climatological analysis of spatially compounding heatwaves and cold spells in the global midlatitudes. Specific geographical areas, such as Western Russia, Central Europe, Southwestern Eurasia and Western North America, emerge as hotspots for concurrent temperature extremes. Concurrent heatwaves are becoming more frequent, longer-lasting and more extended in the Northern Hemisphere, while the opposite holds for concurrent cold spells. Concurrent heatwaves in the Southern Hemisphere are comparatively rare, but have been increasing in both number and extent. Notably, these trends in concurrent temperature extremes are significantly stronger than the corresponding trends in all temperature extremes.

1. Introduction

Extreme climate events often do not occur in isolation, but are triggered by complex processes leading to multiple extremes. An example are events occurring roughly simultaneously at remote locations. These are typically due to specific large-scale atmospheric or oceanic features and are referred to as concurrent, or spatially compounding, extremes (Zscheischler et al., 2020). Temperature extremes often play a prominent role in concurrent events, either in isolation or in conjunction with other extreme event categories. Specific examples in the Northern Hemisphere (NH) include drought–cold spells–wet and windy extremes during winter 2013/14 (Davies, 2015), heatwave–heavy precipitation during summer 2010 (Lau and Kim 2012; di Capua et al., 2021) and concurrent heatwaves and heatwave–heavy precipitation during summer 2018 (Kornhuber et al., 2019). Building upon these episodic events, the literature has considered recurrent spatially compounding extremes, such as wintertime cold–wet–windy extremes in North America and Europe (Messori et al., 2016; Leeding et al., 2023; Riboldi et al., 2023; Messori and Faranda, 2023), and opposite temperature extremes in East Asia and North America (Sung et al., 2021). A parallel line of work has analysed large-scale atmospheric patterns favouring concurrent extremes, highlighting the role of large-amplitude or recurrent atmospheric waves (Coumou et al., 2014; Röthlisberger et al., 2019; Kornhuber et al., 2020; Bui et al., 2022; White et al., 2022; Kornhuber and Messori, 2023). These waves are particularly effective in engendering temperature extremes in both the warm and cold seasons (e.g. Screen and Simmonds, 2014), whose synchronised occurrence triggers detrimental socio-economic and environmental

40   impacts such as widespread crop failures (Tigchelaar et al., 2018; Kornhuber et al., 2020; Gaupp et al., 2020), increased mortality, wildfires, power supply disruptions and more (Vogel et al., 2019).

Previous work on concurrent temperature extremes has often focussed on specific regions or seasons (e.g. Röthlisberger et al., 2019; Kornhuber et al., 2019). More recent work has provided an overview of long-term trends and geographical hotspots of concurrent extremes (Rogers et al., 2022), yet with a focus on NH heatwaves

45   and for a fixed definition of what is "extreme". Broader studies looking at compound extremes or multi-risks have not tailored their analyses and methods specifically to temperature extremes, providing limited flexibility for defining both the extremes themselves and their spatial relation (e.g. Claassen et al., 2023). In this study, we pursue a dual aim. We first introduce a flexible toolbox to compute statistics on concurrent temperature extremes, with adjustable parameters that different users can tailor to their specific needs. While the toolbox was developed

50   specifically for temperature extremes, it can in principle take any single-level variable as input. We then use the toolbox to present a climatological analysis of concurrent hot and cold extremes in both hemispheres.

2. A flexible toolbox for the analysis of concurrent temperature extremes

Input and parameters – Our toolbox takes as input gridded temperature (or temperature anomaly) data on a regular

55   latitude-longitude grid. The users first need to: (i) define a latitudinal domain; (ii) pick a season in the form of a set of months; (iii) choose whether to limit the analysis to land gridpoints or not; and (iv) select a percentile to define the temperature extremes. After this, the toolbox computes the percentile threshold at each gridbox and identifies gridpoints above (for heatwaves) or below (for cold spells) said threshold (Fig. 1a). Next, the users can impose a minimum duration requirement, such that only gridpoints exceeding the threshold over a set number of

60   consecutive days are retained (Fig. 1b).

Clustering and minimum extent – In the following step, the users can flexibly define how to cluster different connected areas of extremely hot or cold gridpoints. Often, one finds a large connected area of extremely hot or cold temperatures, with smaller surrounding areas separated by a few gridpoints from the main area. These are likely caused by the same physical driver(s) as the main connected area. For example, there is no *a priori* reason

65   to believe that two regions of temperature extremes with a one-gridpoint gap in-between should be associated with independent large-scale drivers. The users can decide not to cluster different connected areas, to cluster them based on the distance between the locations of each connected area's centroid, or to cluster them based on the distance between the closest gridboxes of each pair of connected areas. The output of the clustering is a set of well-separated temperature extreme regions (Fig. 1c). We are aware of existing clustering algorithms, which have

70   been used in the context of compound climate extremes (e.g. Tilloy et al., 2022). We do not claim that our algorithm outperforms these, but rather that it provides a more intuitive parameter input set, in terms of type of distance in kilometres (centroids or closest points), as opposed to quantities such as minimum density of points in a given neighbourhood. Finally, the user can impose a minimum areal extent for each clustered temperature extreme region (Fig. 1c). Given that our toolbox does not consider set regions, but rather updates the boundaries

75   of the temperature extremes at every timestep, we do not consider time lags in the compounding, but rather output the statistics at every timestep of our data (see also Rogers et al., 2022, for a similar argument).

We recognise that our toolbox comes with a number of conceptual simplifications, for example by ignoring the shape of the connected extreme temperature areas when performing the clustering (beyond implicitly taking it into account if computing centroids) and by imposing persistence as continuous exceedance of a threshold instead

80 of allowing for discontinuous exceedances clustered in time. These were decided upon to strike a balance between flexibility and interpretability/usability of the toolbox.

a) Define domain, season, threshold and other parameters
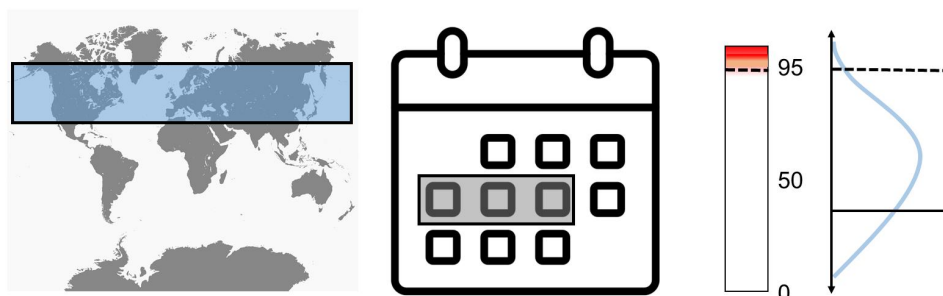
b) Determine minimum duration   c) Cluster and impose minimum extent
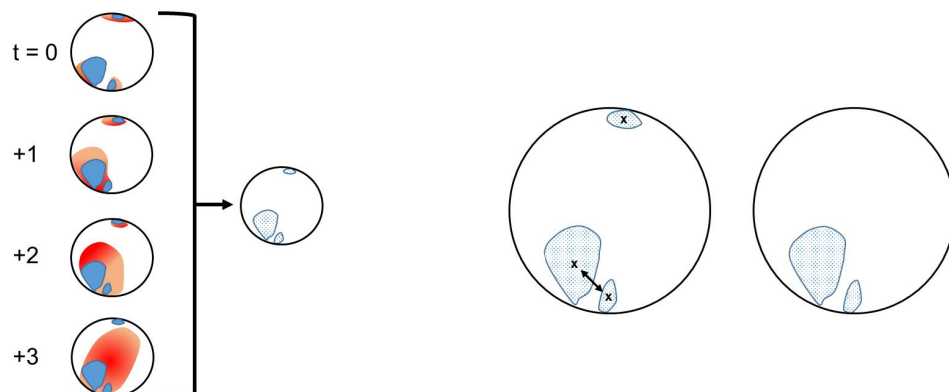
Figure 1: Schematic of the concurrent temperature extremes algorithm. (a) Given a latitudinal domain, a season and a temperature percentile (in the example here, the 95th percentile), the algorithm identifies temperature
85 extremes. (b) A minimum duration in days is then imposed at every location (in the example here, 4 days). The red areas represent percentile exceedances. The overlaid blue shading, regions where the exceedances satisfy the minimum duration. (c) Connected extreme temperature areas are identified (stippled regions), and clustered (in this example using centroid distances, with centroids of each connected area marked by "x"). The two centroids that are clustered are connected by a double-headed arrow. After clustering, a minimum area threshold is applied.
90 The map in (a) is reproduced from FreeVectorFlags.com under an attribution-only licence. The calendar icon in (a) is reproduced from DinosoftLabs under an attribution-only licence.

In the analysis we present in this study, we use daily-mean ERA5 (Hersbach et al., 2020) 2-metre temperature data over 30°–70° N/S in the period January 1940–August 2023, with a horizontal resolution of 0.5° latitude and longitude. However, the toolbox is easily applicable to other gridded climate datasets with different resolutions.

95 We consider non-detrended temperature anomaly data, with anomalies computed relative to a daily climatology smoothed with a 15-day running mean. The toolbox however provides the option to perform a detrending step. We identify hot extremes during summer (boreal: June, July and August – JJA; austral: December, January and February – DJF) and cold extremes during winter (boreal: DJF; Austral: JJA). In Sect. 3, we consider percentile thresholds of 95 (5) for hot (cold) extremes (similar to e.g. Harnik et al., 2016 and Guirguis et al., 2018). We also

100   display results for percentile thresholds of 90 (10) in Appendix A, as these have also often been adopted in the

literature (e.g. Peings et al., 2013; Lin et al., 2022 and Holmberg et al., 2023). The percentiles are applied to the

temperature anomalies at each gridbox. We impose a minimum duration threshold of 4 days, again in line with

previous work that often adopts thresholds of 3–5 days (e.g. Xu et al., 2016; Brown, 2022; Lin et al., 2022), and

show here the results for clustering based on centroid distances below 1000 km. We further enforce a minimum

105   areal extent of clustered temperature extremes of 2×10^5 km^2. This is an intermediate value compared to previous

literature, which has considered thresholds from order 10^5 to order 10^6 km^2 (cf. Lyon et al., 2019 and Rogers et

al., 2022). In general, we do not attempt to provide a full parameter sweep of our toolbox, but rather try to select

values that enable a comparison of our results to previous literature on temperature extremes.

110   ### 3.   A Global Climatology of Concurrent Temperature Extremes

Two clear hotspots for the occurrence of concurrent heatwaves emerge in Western Russia and Western North

America (Fig. 2a), with relative frequencies around or exceeding 0.4. In other words, roughly 40% of single-

gridbox heatwaves at those locations are part of a set of multiple concurrent, large-scale heatwaves across the NH.

Heatwaves in Central Asia and Central North America instead typically occur in isolation. Concurrent cold spells

115   display a different geographical distribution, with Northwestern North America, Central Europe and Southwestern

Eurasia showing the highest relative occurrences (Fig. 2b). At some of these locations, roughly half of the single-

gridbox cold spells are part of a set of multiple concurrent, large-scale events. Concurrent temperature extremes

are rare in relative terms in the Southern Hemisphere (SH), presumably because of the much smaller landmass

extent.
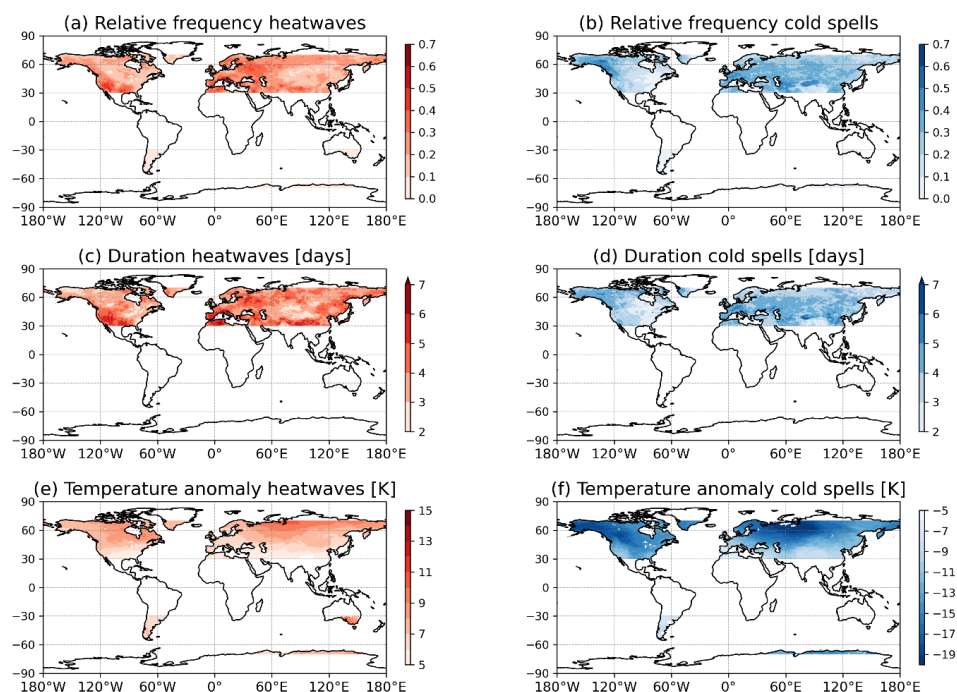
120

Figure 2: Relative frequency, duration and severity of concurrent temperature extremes. Relative frequency of concurrent (a) heatwaves and (b) cold spells, normalised relative to the percentile used to define the extremes. For example, a value of 0.5 means that half of the temperature extremes at a given location concur with another remote temperature extreme of the same sign. Mean duration (days) of concurrent (c) heatwaves and (d) cold spells. Mean temperature anomalies of concurrent (e) heatwaves and (f) cold spells. Panels (e) and (f) have differing colour range amplitudes.

The duration of both concurrent heatwaves and cold spells ranges in most regions between 3 and 6 days. The above-mentioned regional hotspots for occurrence frequency also display slightly above-average duration values. The rare concurrent temperature extremes in the SH show a much shorter duration than their NH counterparts. Note that the duration of a compound temperature extreme can be shorter than the minimum duration threshold imposed for single-gridbox extremes, as here we only count the duration of an extreme while there is at least one other concurrent extreme. The pattern of climatological temperature anomalies during the extremes roughly matches that of the temperature variance (Fig. A1), being largest in the Northern high latitudes and central parts of the continents, and larger for wintertime cold spells than summertime heatwaves. The corresponding results for a less stringent percentile definition of temperature extremes are shown in Fig. A2 and commented on in Appendix A.
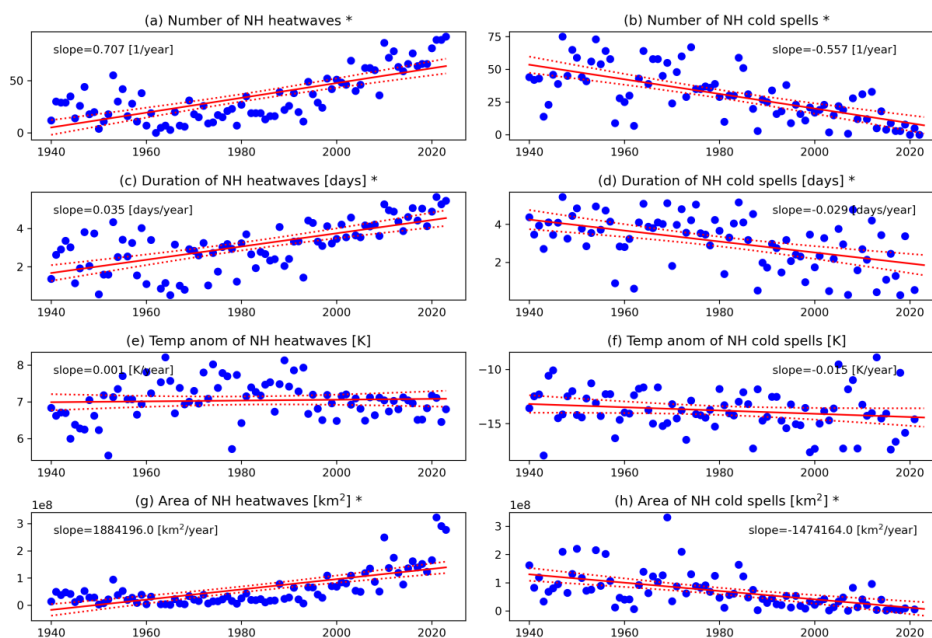
Figure 3: NH aggregated yearly data and trends in the occurrence, duration, severity and extent of concurrent temperature extremes. Number of concurrent (a) heatwaves and (b) cold spells. Mean duration (days) of concurrent (c) heatwaves and (d) cold spells. Mean temperature anomalies (K) of concurrent (e) heatwaves and (f) cold spells. Cumulative area (km^2) of concurrent (g) heatwaves and (h) cold spells. The continuous lines show linear fits, and the dashed lines 95% confidence bounds. The numbers in each panel show the linear fit slope. Asterisks in the panel titles indicate that the slope is different from 0 at the 5% level according to the p-value of the t-statistic. Seasons without any events are not accounted for when computing the linear fits for duration, severity and extent.

This climatology can be compared to that of all temperature extremes, regardless of whether they concur with others or not, but subject to the same percentile, duration and extent thresholds (Fig. A3). The spatial distributions are remarkably similar, with the main difference being that SH temperature extremes emerge more clearly. Moreover, the extremes display a longer duration since this now also includes days when they occur in isolation.

150 We next consider trends in the concurrent temperature extremes, aggregated at hemispheric level (Fig. 3). Concurrent NH heatwaves have significantly increased in number, duration and area over the last 8 decades (Fig. 3a, c, g). As expected given our percentile-based definition, the temperature anomalies associated with the heatwaves have stayed roughly constant (Fig. 3e). Concurrent cold spells show mirror trends, with significant decreases in number, duration and area (Fig. 3b, d, h). The corresponding figures for the SH and for a less stringent

155 percentile definition of temperature extremes are shown in Figs. A4–A6 and commented on in Appendix A.
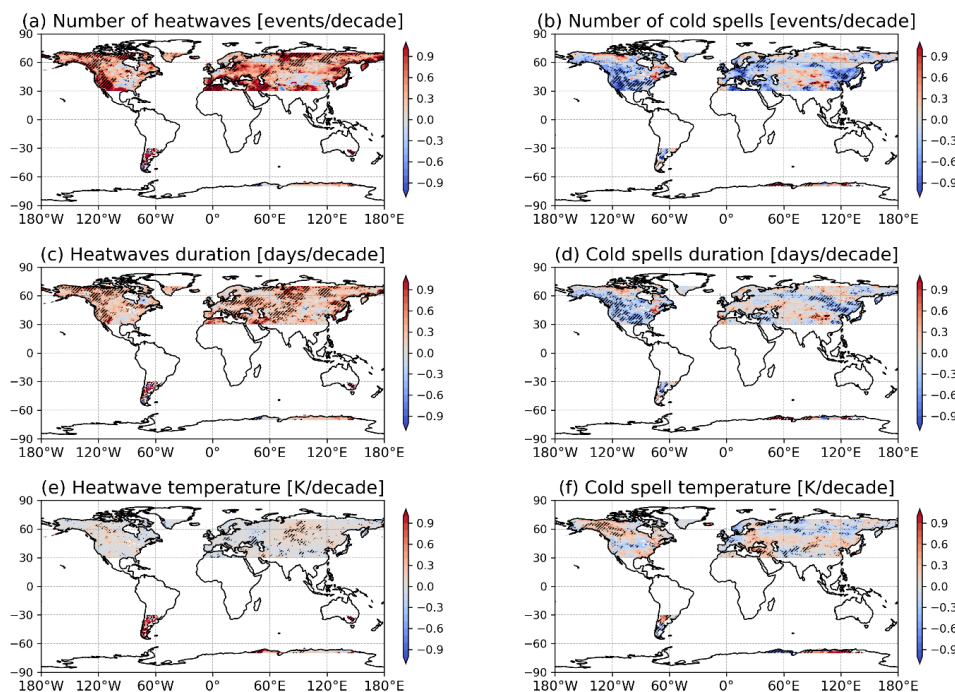
Figure 4: Trends in the occurrence, duration and severity of concurrent temperature extremes. Trends in number of concurrent (a) heatwaves and (b) cold spells; in duration of concurrent (c) heatwaves and (d) cold spells; and in temperature anomalies during concurrent (e) heatwaves) and (f) cold spells. Stippling shows regions where the trends are different from 0 at the 5% level according to the p-value of the t-statistic. A Gaussian filter with filter size 1 has been applied to all panels to improve legibility.

The above trends at hemispheric level can be compared to the corresponding trends for temperature extremes with no requirements for concurrence (Figs. A7, A8). The trends are qualitatively similar, with a marked increase in heatwaves and decrease in cold spells. We additionally see a significant decrease (increase) in NH (SH) cold spell

165 temperature anomalies.

We conclude our analysis by considering trends on a geographical basis (Fig. 4). The frequency of concurrent heatwaves (cold spells) shows a widespread increase (decrease) across the global midlatitudes (Fig. 4a, b). The

hotspot region of Western North America, already highlighted in Fig. 2, emerges as having a particularly strong and geographically widespread increasing heatwave trend. A strong decreasing trend is found for cold spells over

170   the same region. Central Asia and Central North America are exceptions, showing little or even weak negative (positive) changes in the number of concurrent heatwaves (cold spells). The duration trends of concurrent temperature extremes roughly match the occurrence trends, albeit with some regional differences (Fig. 4c, d). For example, Western Russia emerges as having a significant positive duration trend in concurrent heatwaves but no significant occurrence trend. Finally, only a weak signal is seen in the temperature anomaly trends, with the most

175   notable features being positive trends in South America for concurrent heatwaves and positive trends in Northwestern North America for concurrent cold spells. The corresponding figures for a less stringent percentile definition of temperature extremes and for all extremes are shown in Figs. A9 and A10 and commented on in Appendix A.

180   **4.   Concluding Remarks**

We have presented a flexible algorithm for the study of concurrent temperature extremes, and have applied it to cold and hot extremes in the global extratropics. Concurrent temperature extremes affect all land areas, although clear hotspots emerge, for example in Western Russia and Western North America for heatwaves and in Northwestern North America, Central Europe and Southwestern Eurasia for cold spells.

185   Consistent with previous work, we find clear upward trends in concurrent heatwave extent and number (Rogers et al., 2022), while decreasing trends are found for concurrent cold spells. For the concurrent NH heatwaves, the upward trend in occurrence corresponds to more than a quadrupling of events over 8 decades, while concurrent NH cold spells have become rarer by roughly two-thirds. Concurrent temperature extremes have historically mainly occurred in the NH extratropics, due to the much smaller land surface area in the SH. However, the sharp

190   increase in concurrent heatwaves means that these are becoming an emerging hazard in the SH. We further find an increase in duration of concurrent heatwaves and a decrease for concurrent cold spells. In the first decades of the analysis period, concurrent cold spells lasted on average longer than concurrent heatwaves, while the opposite becomes true in the latter part of the analysis period. This is consistent with Lhotka and Kyselý (2015), who found a longer average duration for individual historical cold spells than heatwaves over Europe, and with Allen and

195   Sheridan (2016), who found that in recent decades hot temperatures have on average become longer-lasting than cold temperatures in major U.S. cities. These multi-decadal trends are superimposed on interannual to interdecadal variability, consistent with the know link of several large-scale modes of climate variability with temperature extremes (e.g. Della Marta et al., 2017; Arblaster and Alexander, 2012; Loikith and Broccoli, 2014; Grotjahn et al., 2016, and references therein). On a geographical basis, we find regionally contrasting trends in the number,

200   duration and temperature anomalies of concurrent cold spells in North America and Eurasia. These may be related to the Warm Arctic/Cold Continents pattern (Chen et al., 2018), which also modulates the occurrence of cold extremes (Ye and Messori, 2020). We further find that weaker cold spells show a more uniform decrease than more extreme cold spells (see Appendix A), suggesting that these regional patterns may be sensitive to the definition of extreme events.

205   Nonetheless, caution should be exercised in relating our results on concurrent extremes to those in the literature for extremes without any requirement for concurrence, as the trends can differ markedly. Indeed, the number,

Earth System
Dynamics
Discussions

duration and extent of NH concurrent heatwaves have increased significantly more than the corresponding quantities for all NH heatwaves, and similarly for the decreases in cold spells (Fig. A11).

Given the flexibility of the algorithm presented here, it is our hope that it may be applied to a wide range of
210 datasets, including climate projections, to better quantify the recent and future trends in concurrent temperature extremes and identify specific risk areas. It would be of particular interest to investigate whether the accelerated trends in concurrent temperature extremes relative to all temperature extremes may be associated with dynamical trends associated with climate change. Indeed, a number of studies have found a connection between changes in the atmospheric circulation and regional heatwaves, concurrent heatwaves and long-term temperature trends
215 (Cahynová and Huth, 2016; Rogers et al., 2022; Faranda et al., 2023; Vautard et al., 2023).

Concurrent heatwaves have thus become an increasingly frequent and widespread global hazard. Their increase is faster than that of all heatwaves. Concurrent cold spells show a rapidly decreasing trend, but still occur in the present-day climate.

220 **Appendix A**

We provide below figures corresponding to those shown in the main manuscript, but for a different threshold definition of temperature extremes (Figs. A2, A5, A6, A9); temperature extremes with no requirements for concurrence (Figs. A3, A7, A8, A10); and for the SH (Figs. A4, A6, A8). We further present a map of temperature variance in both the winter and summer seasons in each hemisphere (Fig. A1) and a figure comparing trends in
225 concurrent and all temperature extremes (Fig. A11).

The qualitative features of Fig. 2 as discussed in the main text are reproduced in Fig. A2, although the concurrent temperature extremes display higher relative frequencies, are longer-lasting, and display weaker temperature anomalies. These are intuitive results of including more, weaker events in our analysis.

Due to the small sample size, the only significant trends for the SH concurrent extremes (Fig. A4) are the increases
230 in the number and area of concurrent heatwaves. The results for a less stringent percentile (Figs. A5, A6) reflect those shown in Figs. 3 and A4, albeit with higher numbers and areas of concurrent temperature extremes and weaker average temperature anomalies. Moreover, likely thanks to the larger sample size, we find significant negative trends in the number, duration and extent of SH cold spells.

The key qualitative features of Fig. 4 as discussed in the main text are reproduced in Fig. A9, although in the latter
235 figure the occurrence trends are generally stronger. Moreover, the negative trends in number and duration of cold spells are more geographically uniform. The trends for extremes without any requirement for concurrence (Fig. A10) are generally weaker than those for the concurrent extremes, notably for occurrence and duration.

240
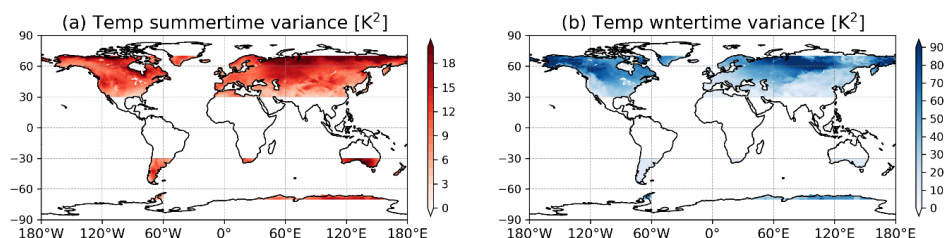
Figure A1: Temperature anomaly variance for (a) summer and (b) winter in each hemisphere. The two panels have differing colour range amplitudes.
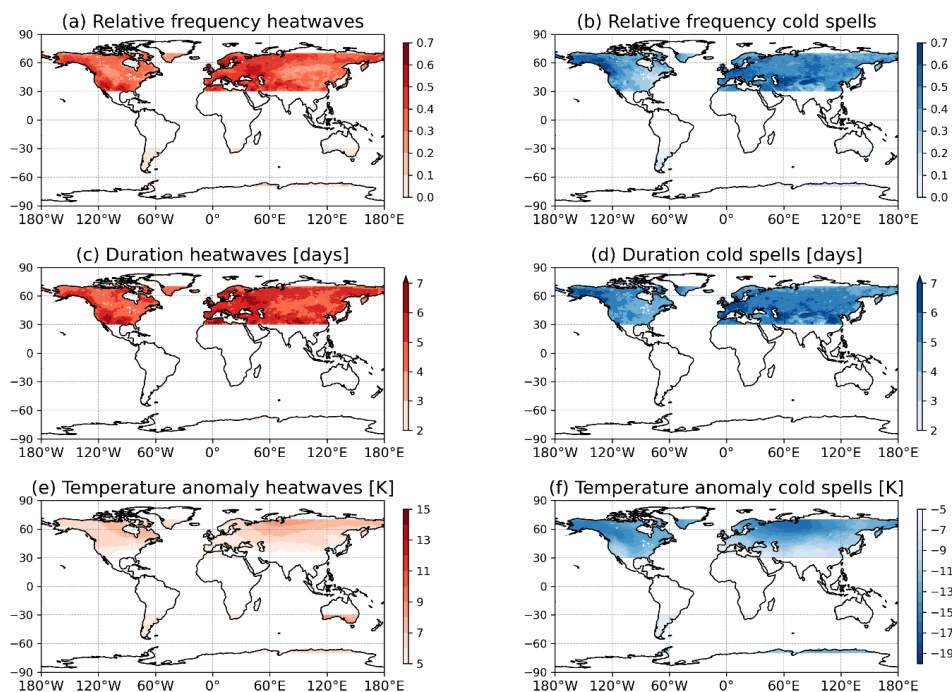
245

Figure A2: As Fig. 2, but for percentile thresholds of 90 (heatwaves) and 10 (cold spells).
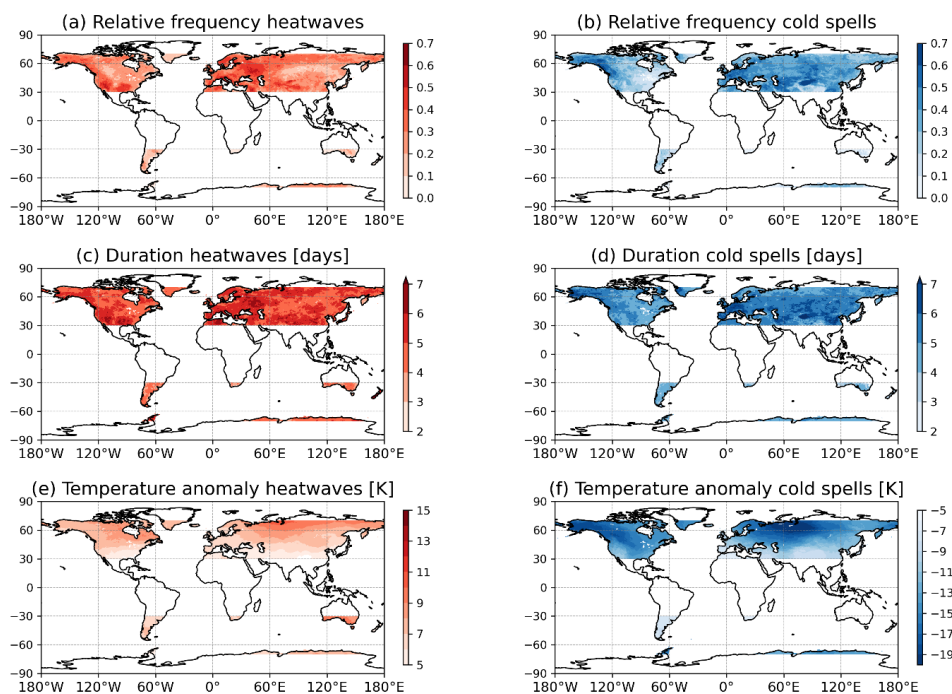
Figure A3: As Fig. 2, but for temperature extremes with no requirements for concurrence.
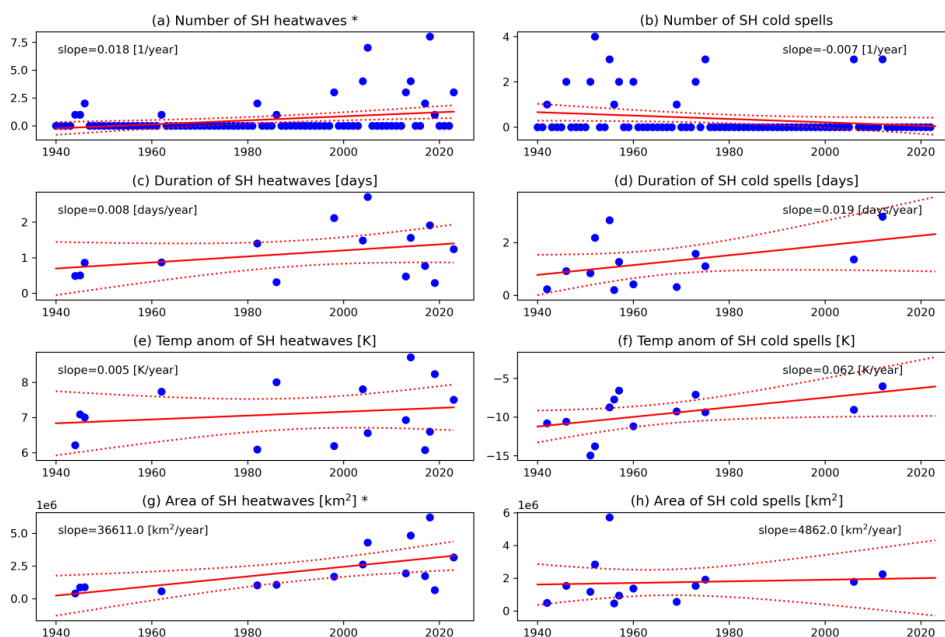
250

Figure A4: As Fig. 3 but for the SH. Seasons without any events are not accounted for when computing the linear fits for duration, severity and extent.
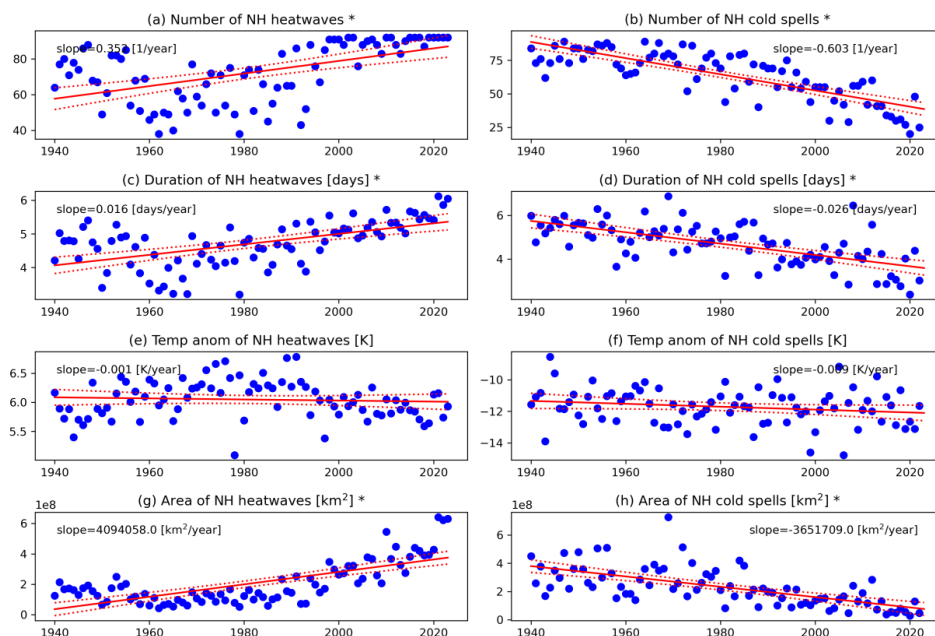
Figure A5: As Fig. 3, but for percentile thresholds of 90 (heatwaves) and 10 (cold spells).

255
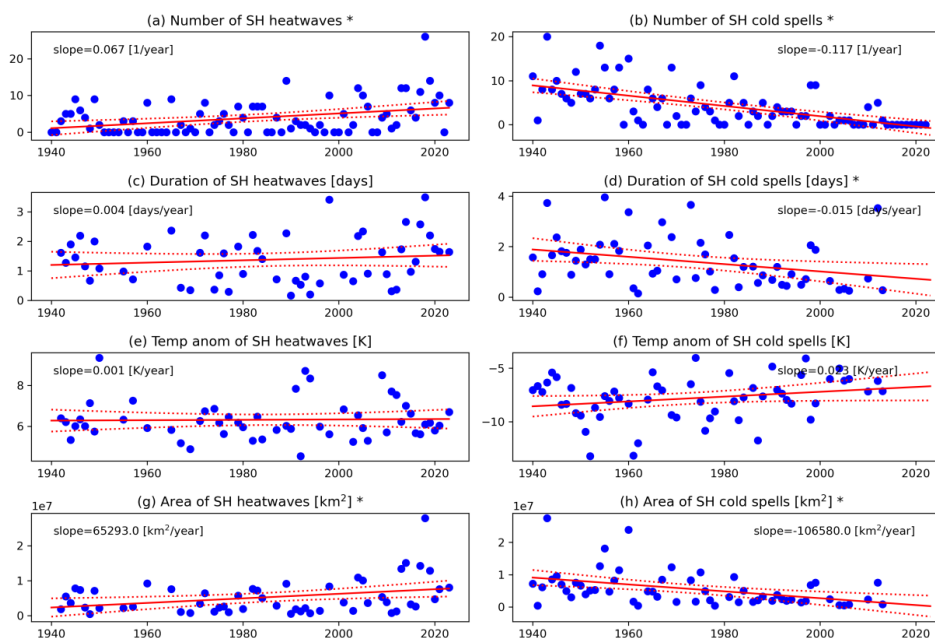
Figure A6: As Fig. A4, but for percentile thresholds of 90 (heatwaves) and 10 (cold spells). Seasons without any events are not accounted for when computing the linear fits for duration, severity and extent.
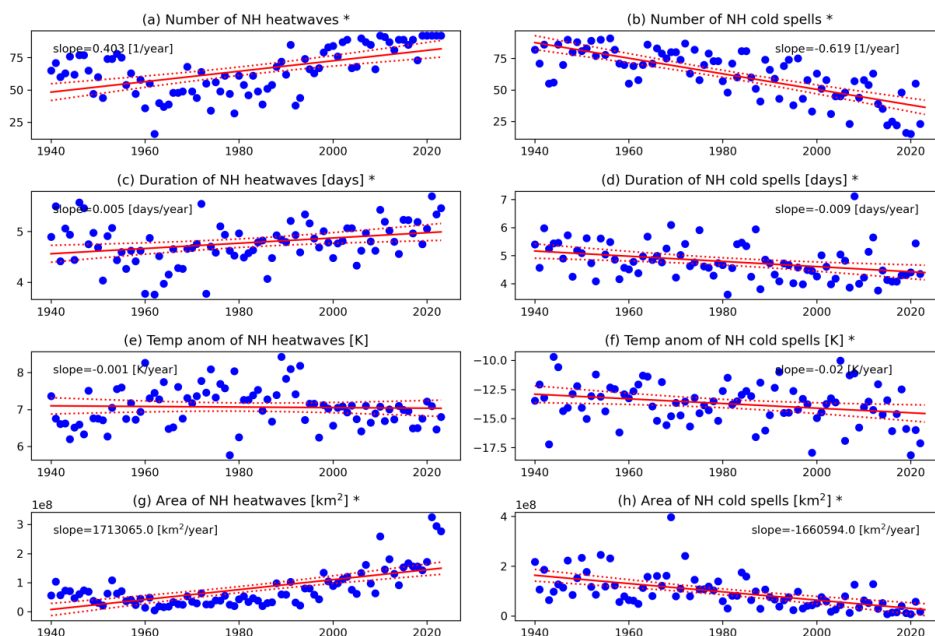
260   **Figure A7:** As Fig. 3, but for temperature extremes with no requirements for concurrence.
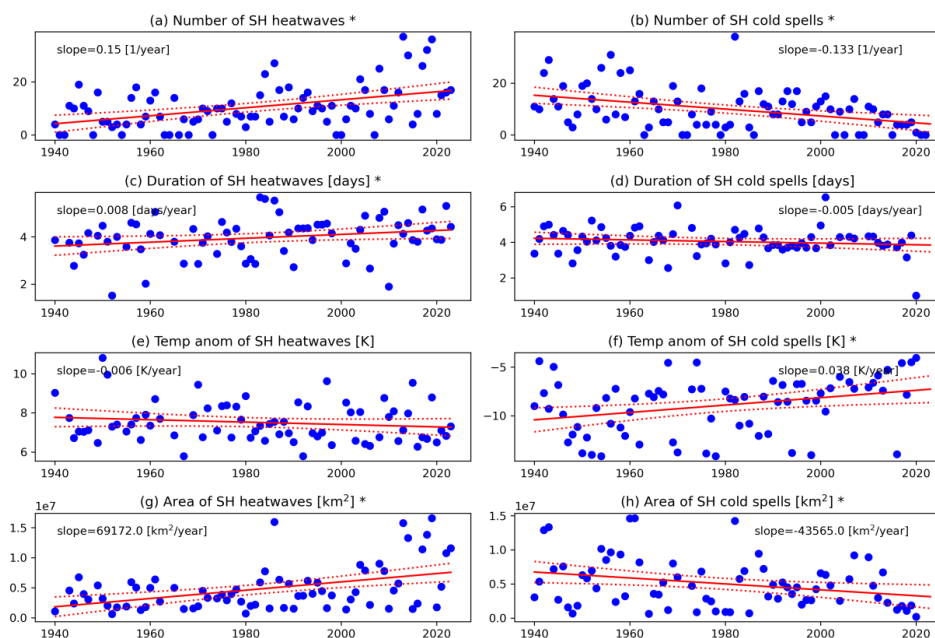
Figure A8: As Fig. A4, but for temperature extremes with no requirements for concurrence. Seasons without any events are not accounted for when computing the linear fits for duration, severity and extent.
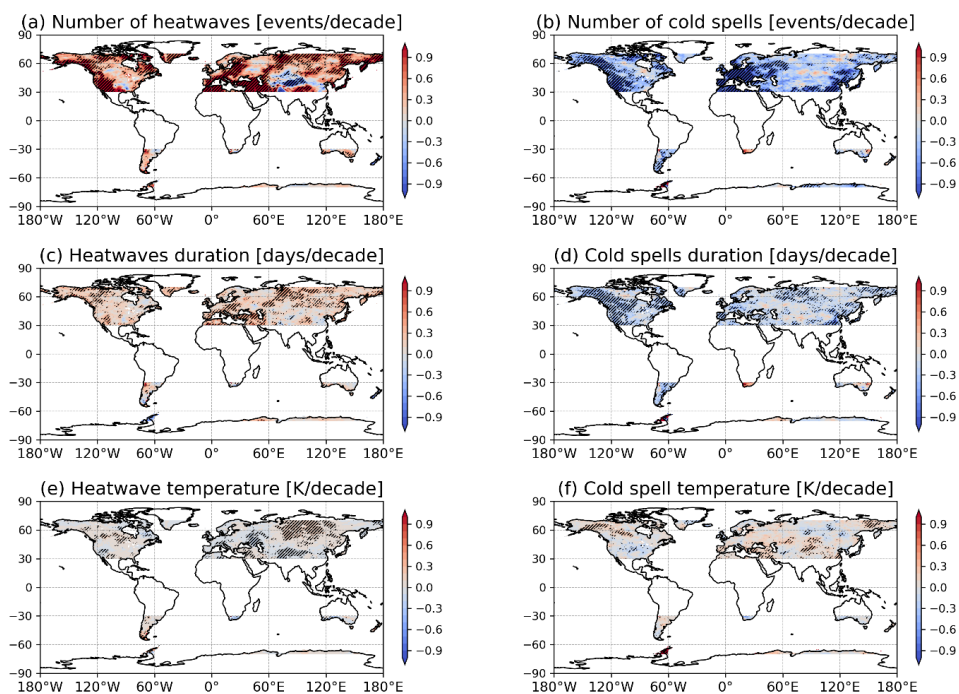
Figure A9: As Fig. 4, but for percentile thresholds of 90 (heatwaves) and 10 (cold spells).
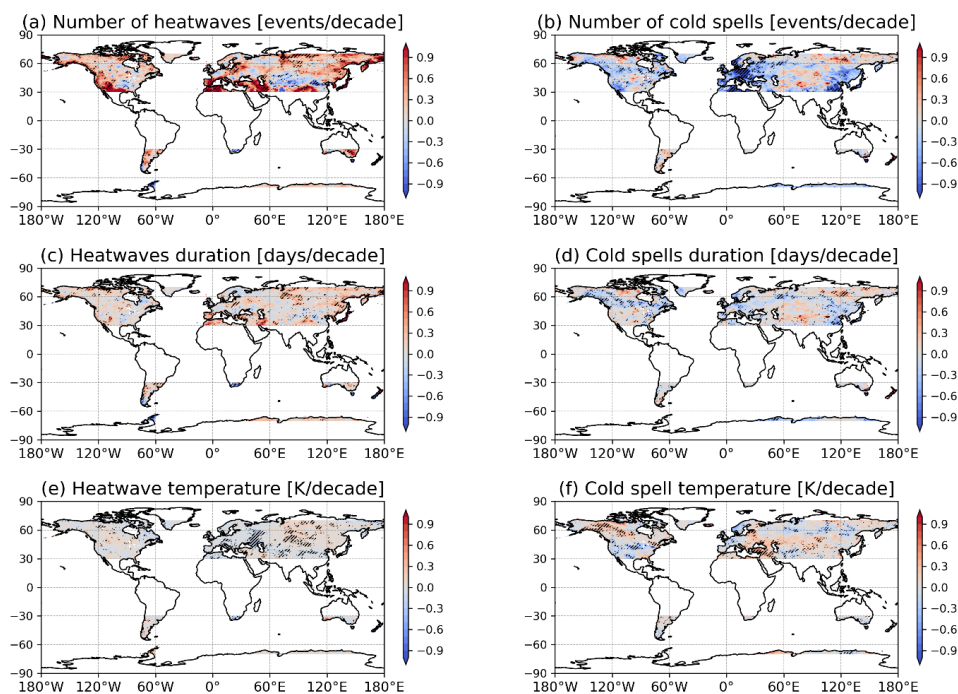
Figure A10: As Fig. 4, but for temperature extremes with no requirements for concurrence.
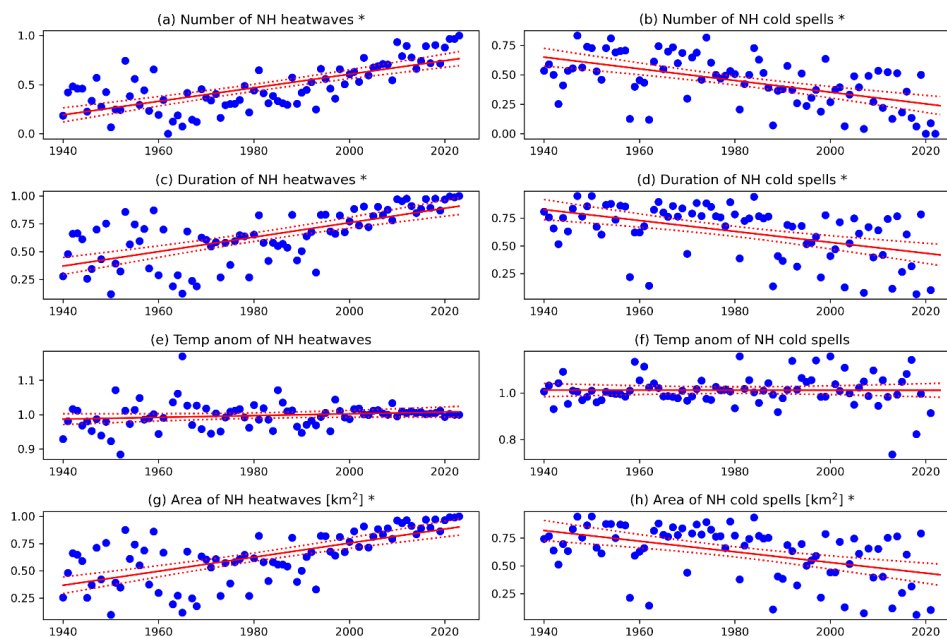
270   **Figure A11:** As Fig. 3, but for the ratio between concurrent temperature extremes and all temperature extremes.

285
References

Allen, M. J., & Sheridan, S. C. (2016). Spatio-temporal changes in heat waves and cold spells: an analysis of 55 US cities. *Physical Geography*, 37(3-4), 189-209.

Arblaster, J. M., & Alexander, L. V. (2012). The impact of the El Niño-Southern Oscillation on maximum temperature extremes. *Geophysical Research Letters*, 39(20).

290

Brown, S. J. (2020). Future changes in heatwave severity, duration and frequency due to climate change for the most populous cities. *Weather and Climate Extremes*, 30, 100278.

Bui, H. X., Timmermann, A., Lee, J. Y., Maloney, E. D., Li, Y. X., Kim, J. E., ... & Wieder, W. R. (2022). Summer midlatitude stationary wave patterns synchronize Northern Hemisphere wildfire occurrence. *Geophysical Research Letters*, 49(18), e2022GL099017.

295

Cahynová, M. and Huth, R. (2016), Atmospheric circulation influence on climatic trends in Europe: an analysis of circulation type classifications from the COST733 catalogue. *Int. J. Climatol.*, 36: 2743-2760. https://doi.org/10.1002/joc.4003

Chen, L., Francis, J., & Hanna, E. (2018). The "Warm-Arctic/Cold-continents" pattern during 1901–2010. *International Journal of Climatology*, 38(14), 5245-5254.

300

Della-Marta, P. M., Luterbacher, J., von Weissenfluh, H., Xoplaki, E., Brunet, M., & Wanner, H. (2007). Summer heat waves over western Europe 1880–2003, their relationship to large-scale forcings and predictability. *Climate Dynamics*, 29, 251-275.

Di Capua, G., Sparrow, S., Kornhuber, K., Rousi, E., Osprey, S., Wallom, D., ... & Coumou, D. (2021). Drivers behind the summer 2010 wave train leading to Russian heatwave and Pakistan flooding. *npj Climate and*
305 *Atmospheric Science*, *4*(1), 55.

Claassen, J. N., Ward, P. J., Daniell, J., Koks, E. E., Tiggeloven, T., & de Ruiter, M. C. (2023). A new method to compile global multi-hazard event sets. *Scientific Reports*, 13(1), 13808.

Coumou, D., Petoukhov, V., Rahmstorf, S., Petri, S., & Schellnhuber, H. J. (2014). Quasi-resonant circulation regimes and hemispheric synchronization of extreme weather in boreal summer. *Proceedings of the National*
310 *Academy of Sciences*, *111*(34), 12331-12336.

Davies, H. C. (2015). Weather chains during the 2013/2014 winter and their significance for seasonal prediction. *Nature Geoscience*, *8*(11), 833-837.

Earth System
Dynamics
Discussions

315   Dole, R., Hoerling, M., Perlwitz, J., Eischeid, J., Pegion, P., Zhang, T., ... & Murray, D. (2011). Was there a basis for anticipating the 2010 Russian heat wave?. *Geophysical Research Letters*, 38(6).

Faranda, D., Messori, G., Jezequel, A., Vrac, M., & Yiou, P. (2023). Atmospheric circulation compounds anthropogenic warming and impacts of climate extremes in Europe. *Proceedings of the National Academy of Sciences*, 120(13), e2214525120.

320   Gaupp, F., Hall, J., Hochrainer-Stigler, S., & Dadson, S. (2020). Changing risks of simultaneous global breadbasket failure. *Nature Climate Change*, *10*(1), 54-57.

Grotjahn, R., Black, R., Leung, R., Wehner, M. F., Barlow, M., Bosilovich, M., ... & Prabhat. (2016). North American extreme temperature events and related large scale meteorological patterns: a review of statistical methods, dynamics, modeling, and trends. *Climate Dynamics*, 46, 1151-1184.

325   Guirguis, K., Gershunov, A., Cayan, D. R., & Pierce, D. W. (2018). Heat wave probability in the changing climate of the Southwest US. *Climate Dynamics*, *50*, 3853-3864.

Harnik, N., Messori, G., Caballero, R., & Feldstein, S. B. (2016). The circumglobal North American wave pattern and its relation to cold events in eastern North America. *Geophysical Research Letters*, *43*(20), 11-015.

Hersbach, H., Bell, B., Berrisford, P., Hirahara, S., Horányi, A., Muñoz-Sabater, J., ... & Thépaut, J. N. (2020). The ERA5 global reanalysis. *Quarterly Journal of the Royal Meteorological Society*, *146*(730), 1999-2049.

330   Holmberg, E., Messori, G., Caballero, R., and Faranda, D. (2023) The link between European warm-temperature extremes and atmospheric persistence, *Earth Syst. Dynam.*, 14, 737–765, https://doi.org/10.5194/esd-14-737-2023.

Kornhuber, K., Osprey, S., Coumou, D., Petri, S., Petoukhov, V., Rahmstorf, S., & Gray, L. (2019). Extreme weather events in early summer 2018 connected by a recurrent hemispheric wave-7 pattern. *Environmental Research Letters*, *14*(5), 054002.

335   Kornhuber, K., Coumou, D., Vogel, E., Lesk, C., Donges, J. F., Lehmann, J., & Horton, R. M. (2020). Amplified Rossby waves enhance risk of concurrent heatwaves in major breadbasket regions. *Nature Climate Change*, *10*(1), 48-53.

Kornhuber, K., & Messori, G. (2023). Recent increase in a recurrent pan-Atlantic wave pattern driving concurrent wintertime extremes. *Bulletin of the American Meteorological Society*, *104*(9), E1694-E1708.

340   Lau, W. K., & Kim, K. M. (2012). The 2010 Pakistan flood and Russian heat wave: Teleconnection of hydrometeorological extremes. *Journal of Hydrometeorology*, *13*(1), 392-403.

Leeding, R., Riboldi, J., & Messori, G. (2023). On Pan-Atlantic cold, wet and windy compound extremes. *Weather and Climate Extremes*, *39*, 100524.

345   Lhotka, O., & Kyselý, J. (2015). Characterizing joint effects of spatial extent, temperature magnitude and duration of heat waves and cold spells over Central Europe. *International Journal of Climatology*, 35(7), 1232-1244.

Lin, C., Kjellström, E., Wilcke, R. A. I., and Chen, D. (2022). Present and future European heat wave magnitudes: climatologies, trends, and their associated uncertainties in GCM-RCM model chains, *Earth Syst. Dynam.*, 13, 1197–1214, https://doi.org/10.5194/esd-13-1197-2022.

350   Loikith P C and Broccoli A J (2014). The influence of recurrent modes of climate variability on the occurrence of winter and summer extreme temperatures over North America *J. Clim.* 27 1600–18

Lyon, B., A. G. Barnston, E. Coffel, and R. M. Horton (2019). Projected increase in the spatial extent of contiguous US summer heat waves and associated attributes. *Environ. Res. Lett.*, **14**, 114029, https://doi.org/10.1088/1748-9326/ab4b41.

355   Messori, G., Caballero, R., & Gaetani, M. (2016). On cold spells in North America and storminess in western Europe. *Geophysical Research Letters*, *43*(12), 6620-6628.

Messori, G., & Faranda, D. (2023). On the systematic occurrence of compound cold spells in North America and wet or windy extremes in Europe. *Geophysical Research Letters*, *50*(7), e2022GL101008.

360 Peings, Y., Cattiaux, J., & Douville, H. (2013). Evaluation and response of winter cold spells over Western Europe in CMIP5 models. *Climate Dynamics*, *41*, 3025-3037.

Riboldi, J., Leeding, R., Segalini, A., & Messori, G. (2023). Multiple Large-Scale Dynamical Pathways for Pan–Atlantic Compound Cold and Windy Extremes. *Geophysical Research Letters*, *50*(10), e2022GL102528.

Rogers, C. D., Kornhuber, K., Perkins-Kirkpatrick, S. E., Loikith, P. C., & Singh, D. (2022). Sixfold increase in 365 historical northern hemisphere concurrent large heatwaves driven by warming and changing atmospheric circulations. *Journal of Climate*, *35*(3), 1063-1078.

Röthlisberger, M., L. Frossard, L. F. Bosart, D. Keyser, and O.Martius (2019). Recurrent synoptic-scale Rossby wave patterns and their effect on the persistence of cold and hot spells. *J. Climate*, 32, 3207–3226, https://doi.org/10.1175/JCLI-D-18-0664.1.

Screen, J. A., & Simmonds, I. (2014). Amplified mid-latitude planetary waves favour particular regional weather 370 extremes. *Nature Climate Change*, *4*(8), 704-709.

Sung, M. K., Son, S. W., Yoo, C., Hwang, J., & An, S. I. (2021). Seesawing of winter temperature extremes between East Asia and North America. *Journal of Climate*, *34*(11), 4423-4434.

Tigchelaar, M., D. S. Battisti, R. L. Naylor, and D. K. Ray (2018). Future warming increases probability of globally synchronized maize production shocks. *Proc. Natl. Acad. Sci. USA*, 115, 6644–6649, 375 https://doi.org/10.1073/pnas.1718031115.

Tilloy, A., Malamud, B. D., and Joly-Laugel, A. (2022). A methodology for the spatiotemporal identification of compound hazards: wind and precipitation extremes in Great Britain (1979–2019), *Earth Syst. Dynam.*, 13, 993–1020, https://doi.org/10.5194/esd-13-993-2022.

Vautard, R., Cattiaux, J., Happé, T. et al. (2023). Heat extremes in Western Europe increasing faster than simulated 380 due to atmospheric circulation trends. *Nat. Commun.* 14, 6803. https://doi.org/10.1038/s41467-023-42143-3

Vogel, M. M., J. Zscheischler, R. Wartenburger, D. Dee, and S. I. Seneviratne (2019). Concurrent 2018 hot extremes across Northern Hemisphere due to human-induced climate change. *Earth's Future*, 7, 692–703, https://doi.org/10.1029/2019EF001189.

White, R. H., Kornhuber, K., Martius, O., & Wirth, V. (2022). From atmospheric waves to heatwaves: A 385 waveguide perspective for understanding and predicting concurrent, persistent, and extreme extratropical weather. *Bulletin of the American Meteorological Society*, *103*(3), E923-E935.

Xu, Z., FitzGerald, G., Guo, Y., Jalaludin, B., & Tong, S. (2016). Impact of heatwave on mortality under different heatwave definitions: a systematic review and meta-analysis. *Environment International*, 89, 193-203.

Ye, K., & Messori, G. (2020). Two leading modes of wintertime atmospheric circulation drive the recent warm 390 Arctic–cold Eurasia temperature pattern. *Journal of Climate*, 33(13), 5565-5587.

Zscheischler, J., Martius, O., Westra, S., Bevacqua, E., Raymond, C., Horton, R. M., ... & Vignotto, E. (2020). A typology of compound weather and climate events. *Nature Reviews Earth & Environment*, *1*(7), 333-347.